Available online at www.sciencedirect.com
ScienceDirect
Applied Surface Science 253 (2007) 6382–6385
applied surface science
www.elsevier.com/locate/apsusc

Computational investigation into the mechanisms of UV ablation of poly(methyl methacrylate)

Manish Prasad *, Patrick F. Conforti, Barbara J. Garrison, Yaroslava G. Yingling [1]

Department of Chemistry, 104 Chemistry Building, The Pennsylvania State University, University Park, PA 16802, USA

Available online 26 January 2007

Abstract

Molecular dynamics simulations with an embedded Monte Carlo based reaction scheme were used to study UV ablation of poly(methyl methacrylate) (PMMA) at 157 nm. We discuss the onset of ablation, the formation and distribution of products in the plume and stress relaxation of the polymer matrix. Laser induced heating and bond-breaks are considered as ablation pathways. We show here that depending on the nature of energy deposition the evolution of ablation plume and yield composition can be quite different. If all of photon energy is converted to heat it can set off ablation via mechanical failure of the material in the heated region. Alternatively, if the photon energy goes towards breaking bonds first, it initiates chemical reactions, polymer unzipping and formation of gaseous products inside the substrate. The ejection of these molecules has a hollowing out effect on the substrate which can lead to ejection of larger chunks. No excessive pressure buildup due to creation of gaseous molecules or entrainment of larger polymer chunks is observed in this case.

Keywords: Computational investigation; Mechanisms of UV ablation; Poly(methyl methacrylate)

1. Introduction

Laser ablation of polymeric material is of technological interest with applications ranging from spectroscopy, biomedical diagnostics and treatment to fabrication of materials based on nanotechnology [1–4]. These applications employ lasers over a wide range of operating conditions such as wavelengths, fluences, pulse widths, repetition rates, etc. The plurality of process parameters and varying material properties (both with type of materials and upon application of laser) lead to various kinds of behavior during the laser ablation process [5–12]. Typically, laser irradiation of a material causes electronic excitation of atoms, possibly followed by bond cleavage, desorption, chemical reactions, propagation of stress waves and/or bulk ejection of material. A detailed and quantitative understanding of ablation physics is necessary to further optimize and develop these applications.

In this paper, we perform molecular dynamics (MD) simulation of laser irradiation of PMMA over a small set of these process conditions. We explore different photo-excitation pathways available to the PMMA matrix and their influence on the polymer substrate, plume and the yield. Previously, two broad classes have been proposed: photothermal and photochemical [5,13–15]. In the case of ''pure'' photothermal excitation, the photon energy is absorbed at specific sites (chromophores) along the polymeric chains. This energy is subsequently converted into heat, which may produce high temperature in the absorbing region leading to thermal degradation of the material and high mechanical stresses causing massive ejection of material or ablation [6,7]. Alternatively, in ''pure'' photochemical excitation scenario, photon energy is utilized to break bonds at absorption sites. This photo-fragmentation creates radicals and new molecular entities by chemical reactions and possibly ablation [5,16,17].

In a realistic system, the actual process dynamics are rather complex with all possible pathways contributing to varying extents. The aim of this initial study is not to mimic a realistic system. Instead, our aim here is to ascertain contributions made by these different pathways that can set off ablation. It is believed that in the photothermal case the cause of massive

* Corresponding author.
E-mail address: manishp@psu.edu (M. Prasad).
[1] Present address: Center for Cancer Research Nanobiology Program, National Cancer Institute, National Institute of Health, Frederick, MD 21702, USA.

0169-4332/$ – see front matter © 2007 Elsevier B.V. All rights reserved.
doi:10.1016/j.apsusc.2007.01.054

ejection is mechanical in nature whereas in the photochemical case it is the pressure developed by creation of small molecules that drives the ablation [5,9].

2. Simulation details

The PMMA substrate consists of 951 polymeric chains of 19 monomeric units each in amorphous state. The sample was prepared according to the method described in Refs. [18,19]. Each chain itself was made up of coarse grained ''beads'' or super-atoms which represent a functional group [20]. For PMMA, these groups are CH_x ($0 \leq x \leq 3$), CO and O. The bonding and angular potentials were taken from Ref. [21] and the non-bonded Morse potential was fitted to match PMMA physical properties like cohesive energy [20]. Each simulation was started with initial temperature of 300 K and density of 1.2 gm/cm^3 (51 Å × 51 Å × 936 Å). The laser pulse of wavelength (λ), pulse width (τ) and penetration depth ($1/\alpha$), was applied to the sample from $t = 0$ to $t = \tau$. The photons are absorbed by the chromophores (–C– or –CO– in this case) in accordance with Beer's law. In the pure photothermal or heating case, photon energy is distributed over a monomeric unit (six beads) as kinetic energy. In the photochemical case photon energy is utilized to break two types of bonds. In the first case, called Norrish type I reaction. The –C–CO– bond on a PMMA side chain is broken. In Norrish type II reaction, –C–CH_2– bond on a polymer's main chain is broken. The excess photon energy goes to heat the beads involved in bond break. The detailed simulation methodology will be described elsewhere [22]. Also, periodic boundary conditions were applied to the sides and pressure absorbing boundary condition was applied at the bottom of the sample to prevent the downward traveling pressure wave from reflecting back into the sample [23].

Formation of radicals in the substrate leads to chemical reactions which are believed to play an important role in ablation as mentioned above. These reactions occur based on a Monte Carlo scheme with predetermined Arrhenius reaction rates and formation energies [22,24]. They are performed during the MD simulation using a modified version of the coarse grain chemical reaction model (CGCRM) [20,25]. Upon bond break, radicals can undergo reactions causing polymer unzipping, hydrogen abstraction and formation of CO, CO_2, CH_4, $HCOOCH_3$ and CH_3OH, details of which will be described elsewhere [22]. In the heating case, bonds were allowed to stretch and break (due to high thermal energy), but they were not explicitly labeled as radicals and therefore no subsequent chemical reaction takes place.

Ablation simulations were performed at $\lambda = 157$ nm (7.9 eV/photon) over fluence ranging from 2 to 20 mJ/cm^2. The pulse width studied were $\tau = 100$ femto-seconds (fs) and $\tau = 5$ pico-seconds (ps). The penetration depth was set at 100 Å. The 157 nm laser, short pulse width and small penetration depth were chosen to maximize ablation yield and any observable phenomena associated with it. The simulations were followed over a period of 500–1000 ps depending on evolution of ablation yield over time.

3. Simulation results and discussion

The ablation yields as a function of laser fluences for the three different cases: heating, Norrish type I reactions and Norrish type II reactions are shown in Fig. 1. For each of the three cases (with $\tau = 5$ ps), the ablation threshold lies between 5 and 10 mJ/cm^2 when the yields jump above a 1000 MMA units. This rise in yield is steep in this range as below 8 mJ/cm^2 it falters to a few MMA units while above 15 mJ/cm^2 it saturates. All the three cases follow a similar trend and the yield in each case is not much different from others. Similar results are obtained at 100 fs pulse width case (not shown), which establishes that yield is not a function of the pulse width for short pulse widths. However, the effect of much longer pulse width (~100 ps or more) is not known and is under investigation. The average size of ejected clusters in these cases is also shown in Fig. 1. The clusters are identified by grouping together all the coarse-grained beads found within a distance of 5 Å of each other. Average size is then computed as ratio of second moment of cluster size distribution over its first moment. As can be seen, the average cluster size also rises steeply as ablation sets in corresponding to massive ejection of material. It is largest in the pure heating case while the photo-fragmentation cases yield much smaller clusters. Moreover, the clusters in the first case are stable in size and do not fragment once they are ejected, while the clusters in latter two cases are dynamically evolving, rapidly fragmenting into smaller units as shown in a snapshot of these three simulations in Fig. 2. Further analysis of the yielded products and the substrate brings out many differences in the way ablation is reached in each of the three cases.

In the case of pure heating, fluences below the 8 mJ/cm^2 threshold results in little swelling and the yield is comprised mostly of desorbed monomers. For fluences greater than 8 mJ/cm^2, heat deposited in the top layers causes generation of a pressure wave which travels in both directions. The substrate swells anywhere from 100 to 200 Å with the surface temperature ranging between 4100 and 4500 K within first

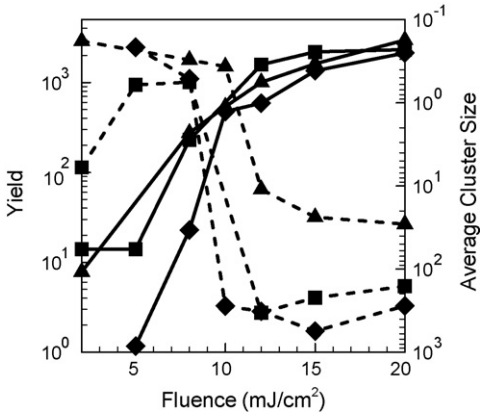

Fig. 1. Yield (solid line) and average cluster size (dashed lines) expressed in number of MMA units as a function of fluence for simulations with $\lambda = 157$ nm, $\tau = 5$ ps and 100 Å penetration depth. The results are for pure heating (diamonds), pure Norrish type I reactions (triangles) and pure Norrish type II reactions (squares).

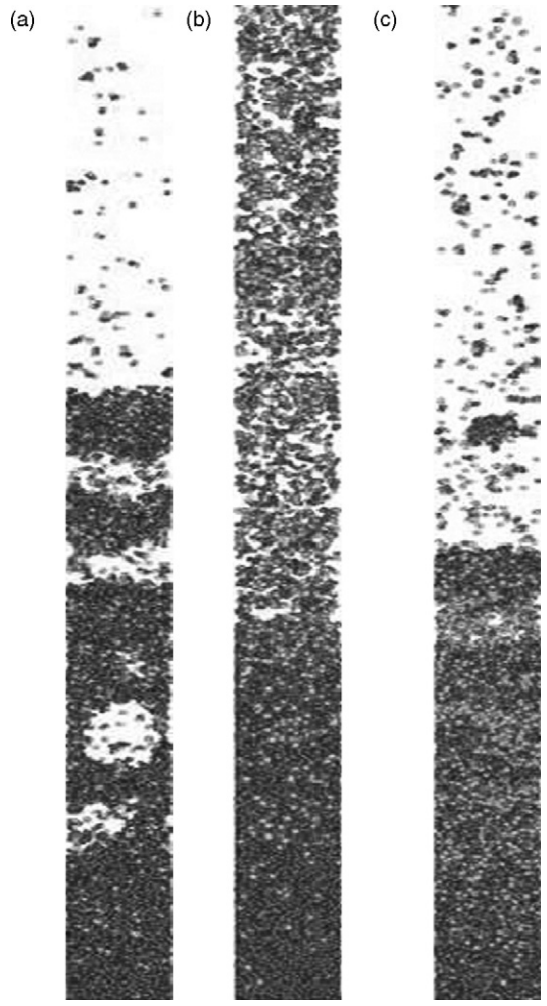

Fig. 2. Snapshots from simulations for the three different cases: (a) heating (at 40 ps), (b) Norrish type I reactions (at 250 ps) and (c) Norrish type II reactions (at 200 ps). The fluence is 20 mJ/cm^2 and the rest of the simulation parameters are same as those given in Fig. 1 The darker circles correspond to coarse-grained beads in original polymer molecules, whereas the lighter ones represent gas molecules and beads with bond lengths stretched over 5 Å.

20–30 ps. High temperature and pressure also forces mechanical breaking of bonds as they get stretched far beyond their equilibrium values. The swelling is a result of expansion following the buildup of excess compressive stress. Ablation occurs at the end of this short time period when a large superhot chunk breaks off the surface (Fig. 2) as the density in top layers drops below 50% of the starting PMMA density. This expansion makes way for tensile stress and causes mechanical failure or spallation. Once ejected the rest of the substrate is substantially cooler with temperatures below 2700 K. The desorption processes continues to eject smaller clusters over a period of 300–500 ps further cooling the substrate to about 2000–2200 K.

For Norrish type I reactions only, once again there is little swelling below the threshold. It is worth noting here that for 157 nm laser pulses a substantial amount of photon energy (about 4 eV) is left over following Norrish type bond break (in both cases) which gets distributed as heat, so these scenarios are far from being purely photochemical in nature. Further studies are being carried out with longer wavelengths to address this issue. Above 8 mJ/cm^2, this residual heat results in 50–120 Å swelling of the substrate (smaller than in the heating case). This swelling however is not sufficient to cause ablation. The newly formed radicals start reacting within the substrate. In the case of Norrish type I bond break, the $^{\bullet}COOCH_3$ radical can form $HCOOCH_3$, or undergo decarboxylation to give CO_2 (exothermic) and $^{\bullet}CH_3$ radical which can form CH_4, or it can break into CO (endothermic) and $^{\bullet}OCH_3$ radical which can form CH_3OH. The distribution of these species was analyzed by dividing the substrate in slices, each 10 Å in depth. It was found that most of these small molecules are formed quickly within first 10–20 ps after bond break and even below the ablation threshold. For example, at 2 mJ/cm^2 the number of CO_2 molecules in top 100 Å ranged from 16 to 46 which stays constant, i.e. these molecules do not eject, whereas at 20 mJ/cm^2 this number is initially at 35–116 over the top 400 Å and drops down to 30–50 at the end of the simulation. The analysis of the yield reveals that CO_2 molecules form about 50% (and $^{\bullet}CH_3/CH_4$ another 25%) of the total (number) yield at 8 mJ/cm^2 dropping to 22% at 20 mJ/cm^2. Carbon monoxide is only formed during the initial stage and in smaller quantities at about 20% of molecular yield of CO_2. The CO yield stays constant as a fraction of the CO_2 yield. The exothermicity of reactions (e.g. CO_2 formation) releases additional heat which contributes to substrate heating and swelling throughout the simulation. The number of radicals ejected goes up from 3 to 28% as the fluence rises from 8 to 20 mJ/cm^2. It is very likely that these radicals will undergo further reactions to form more small molecules over the course of time. Also worth noting is that while just above ablation threshold almost all ejected species are small molecules, with increasing fluence their proportion goes down and larger polymer chains constitute the bulk of ablated material.

In the case of Norrish type II reactions, the swelling behavior is similar to that of Norrish type I reactions. Here, the bulk of the yield above the ablation threshold is comprised of unzipped MMA units. These form between 55 and 60% of ejected particles and thermally broken polymer fragments form another 12–15% over the entire fluence range (8–20 mJ/cm^2). The unzipping reaction continues well in to 400–600 ps time range generating MMAs with the substrate temperature in top layers above 2500 K. A consequence of this is that while ablation in previous two cases occurs within first 30–200 ps, here it goes on until 700–900 ps. This continued generation of MMAs is a direct consequence of absence of termination reactions for main chain radicals ($^{\bullet}C$– and $^{\bullet}CH_2$–). Further studies are being carried out after incorporating termination reactions proposed by Stuke and co-workers [17].

The ablation mechanisms in the last two cases involving Norrish type reactions appear to be similar. Once small molecules reach a critical bulk density they start streaming out of the sample which over time leads to hollowing out of the sample. The hollowed out sample ejects larger chunks which tend to fragment soon after ejecting. The hollowing out effect is much pronounced in Norrish type II reactions, because it breaks the main chain of the polymer. We do not observe any

significant compressive pressure buildup in the substrate following creation of small molecules. It is likely small pressure fluctuations are enough to dislodge large polymer fragments off the hollowed out top layers. Maximum escape velocities for smaller clusters (size < 10) are in the vicinity of 2000 m/s, while larger chunks break off at much lower speeds suggesting no entrainment/liftoff of larger fragments with smaller ones.

4. Conclusions

The gaseous products observed during our simulations have been reported previously in various laser ablation experiments with PMMA using 157–308 nm wavelength lasers and direct photo-excitation studies [5,9,11,12,26] with differing accounts of the causes of ablation. We have shown here that characteristics of energy deposition greatly alter the composition of ablation plume as well as mechanisms responsible for ablation. Rapid laser heating is shown to set off ablation by mechanical spallation of the polymer matrix whereas laser induced bond breaks acts as basis of formation of small molecules which gets ejected. This gas formation has a hollowing out effect on the substrate, weakening it and leading it to eject. Similar studies of other aspects of ablation coupled with experiments can pave way towards understanding the full range of mechanisms at work.

Acknowledgements

This work was supported by the National Science Foundation through the Information Technology Research Program and the US Air Force Office of Scientific Research through the Multi-University Research Initiative. The computer support was provided by the Academic Services and Emerging Technologies at Penn State University.

References

[1] F. Hillenkamp, M. Karas, Int. J. Mass Spectrom. 200 (2000) 71.
[2] R.E. Johnson, in: T. Baer, C.Y. Ng, I. Powis (Eds.), Large Ions: Their Vaporization, Detection and Structural Analysis, John Wiley, New York, 1996, p. 49.
[3] N.H. Niemz, Laser tissue interactions: fundamentals and applications, in: E. Greenbaum (Ed.), Biological and Medical Physics, Springer, Berlin, 2002, p. 303.
[4] P.E. Dyer, Appl. Phys. A 77 (2003) 167.
[5] R. Srinivasan, B. Braren, D.E. Seeger, R.W. Dreyfus, Macromolecules 19 (1986) 916.
[6] N. Bityurin, A. Malyshev, J. Appl. Phys. 92 (2002) 605.
[7] N. Bityurin, A. Malyshev, B. Luk'yanchuk, S. Anisimov, D. Bauerle, Proc. SPIE 2802 (1996) 102.
[8] T. Lippert, M. Hauer, C.R. Phipps, A. Wokaun, Appl. Phys. A 77 (2003) 259.
[9] D.J. Krajnovich, J. Phys. Chem. A 101 (1997) 2033.
[10] T. Efthimiopoulos, C. Kiagias, G. Heliotis, E. Helidonis, Can. J. Phys. 78 (2000) 509.
[11] T.H. Fedynyshyn, R.R. Kunz, R.F. Sinta, R.B. Goodman, S.P. Doran, J. Vac. Sci. Technol. B 18 (2000) 3332.
[12] M. Tsunekawa, S. Nishio, H. Sato, J. Appl. Phys. 76 (1994) 5598.
[13] N. Bityurin, B.S. Luk'yanchuk, M.H. Hong, T.C. Chong, Chem. Rev. 103 (2003) 519.
[14] H. Schmidt, J. Ihlemann, B. Wolff-Rottke, K. Luther, J. Troe, J. Appl. Phys. 83 (1998) 5458.
[15] T. Lippert, J.T. Dickinson, Chem. Rev. 103 (2003) 453.
[16] R. Srinivasan, B. Braren, Chem. Rev. 89 (1989) 1303.
[17] S. Kuper, M. Stuke, Appl. Phys. A-Mater. Sci. Process. 49 (1989) 211.
[18] N.F.A. vanderVegt, W.J. Briels, M. Wessling, H. Strathmann, J. Chem. Phys. 105 (1996) 8849.
[19] S.B. Sane, T. Cagin, W. Knauss, W.A. Goddard III, J. Comput. Aided Mater. Des. 8 (2001) 87.
[20] Y.G. Yingling, B.J. Garrison, J. Phys. Chem. B 109 (2005) 16482.
[21] W.K. Kim, L.M. Hayden, J. Chem. Phys. 111 (1999) 5212.
[22] M. Prasad, P.F. Conforti, B.J. Garrison, in preparation.
[23] L.V. Zhigilei, B.J. Garrison, Mater. Res. Soc. Symp. Proc. 538 (1999) 491.
[24] P.F. Conforti, B.J. Garrison, Chem. Phys. Lett. 406 (2005) 294.
[25] Y.G. Yingling, B.J. Garrison, J. Phys. Chem. B 108 (2004) 1815.
[26] R.C. Estler, N.S. Nogar, Appl. Phys. Lett. 49 (1986) 1175.